Acta Pharmaceutica Sinica B 2019;9(3):545–556

Chinese Pharmaceutical Association
Institute of Materia Medica, Chinese Academy of Medical Sciences

Acta Pharmaceutica Sinica B

www.elsevier.com/locate/apsb
www.sciencedirect.com

ORIGINAL ARTICLE

# Bioactive A-ring rearranged limonoids from the root barks of *Walsura robusta*

**Faliang An, Xiaobing Wang, Minghua Yang, Jun Luo*, Lingyi Kong***

*Jiangsu Key Laboratory of Bioactive Natural Product Research and State Key Laboratory of Natural Medicines, Department of Natural Medicinal Chemistry, China Pharmaceutical University, Nanjing 210009, China*

Received 22 November 2018; received in revised form 18 January 2019; accepted 15 February 2019

**KEY WORDS**

*Walsura robusta*;
limonoid;
Neotecleanin-type;
ECD spectrum calculation;
Single-crystal X-ray diffraction;
Anti-inflammatory activity;
*Propionibacterium acnes*;
THP-1 human monocytic cell

**Abstract** Screening active natural products, rapid identification, and accurate isolation are of great important for modern natural lead compounds discovery[1]. We hereby reported the isolation of seven new neotecleanin-type limonoids (**1**–**7**), seven new limonoids with 5-oxatricyclo[5.4.0.1$^{1,4}$]hendecane ring system (**8**–**14**), and two new precursors (**15**–**16**) together with four known limonoids (**17**–**20**) from the root barks of *Walsura robusta*. Their structures, including their absolute configurations, were elucidated based on analyses of HR-ESI-MS, 1D/2D NMR, ECD spectrum calculations and single-crystal X-ray diffraction techniques. Compounds **2**, **8**, **9**, **11**, **13**, **14**, **18** showed significant anti-inflammatory activities in LPS-induced RAW 264.7 cell line, BV2 microglial cells, and *Propionibacterium acnes*-stimulated THP-1 human monocytic cells. Walrobsin M (**11**) exhibited anti-inflammatory activity with $IC_{50}$ value of 7.96 ± 0.36 μmol/L, and down-regulated phosphorylation levels of ERK and p38 in a dose-dependent manner.



*Corresponding authors. Fax: +86 25 83271402, +86 25 83271405.
E-mail address: cpu_lykong@126.com (Lingyi Kong), luojun@cpu.edu.cn (Jun Luo).

Peer review under responsibility of Institute of Materia Medica, Chinese Academy of Medical Sciences and Chinese Pharmaceutical Association.

https://doi.org/10.1016/j.apsb.2019.02.009

## 1. Introduction

Natural products (secondary metabolites) revealing interesting properties as complex molecules and/or are widely recognized as an excellent source for target drug candidate discovery[1]. Plants of the genus *Walsura* from Meliaceae[2] are rich sources of bioactive limonoid derivatives with complex and diverse structures[3–9]. Three *Walsura* species are widely distributed in south of China, such as Yunnan, Guangxi, and Hainan provinces[10,11]. In recent years, the studies of *Walsura* species discovered some biologically active limonoids with unprecedented carbon skeletons, such as antimalarial walsuronoid A[12], 11$\beta$-HSD1-inhibited walsucochinoids D and E[7], neuroprotective walsucochins A and B[13] and anti-inflammatory walrobsins A and B[10]. In recent years, more and more new limonoids from *Walsura* genus have been reported. However, few A/B spiro-type limonoids with significant anti-inflammatory activities were reported. High abundances of cedrelone type limonoid and low abundances of A/B spiro-type limonoid have made research on these compounds difficult[3,4,11]. In our previous study, two novel limonoids with unprecedented 5-oxatricyclo[5.4.0.1[1,4]]hendecane ring system were isolated and reported, and walrobsin A showed significant anti-inflammatory activity by inhibiting the expression of iNOS and IL-1$\beta$[10]. In our efforts to discover novel bioactive limonoids in *Walsura*, we decided to rapidly filter "impurious"[14–16] limonoids and targeted the A/B spiro-type limonoids based on the characteristic ultraviolet absorption distinction between cedrelones, including cedrelone, 11$\beta$-acetoxycedrelone, 11$\beta$-hydroxycedrelone (Supporting Information Fig. S1) and walrobsins to guide the isolation based on HPLC–DAD method for the first time.

In this study, four types of A-ring rearranged limomoids were isolated and identified, including 8 neotecleanin-type limonoids (7 new compounds **1**–**7**, and a known compound **17**), 9 limonoids with 5-oxatricyclo[5.4.0.1[1,4]]hendecane ring system (7 new compounds **8**–**14**, and 2 known compounds **18** and **19**), and 2 key new precursors (**15**–**16**) together with the first known limonoid peroxide (**20**) (Fig. 1). Their planar structures, relative configurations and absolute configurations were assigned by comprehensive comparisons and analyses of NMR, HR-ESI-MS and X-ray crystallography. Compounds **1**–**3**, **8**–**14**, and **18**–**20** were screened their inflammatory activities in three models including LPS-induced RAW 264.7, BV2 and *Propionibacterium acnes*-stimulated THP-1 cell lines. Walrobsin M (**11**) exhibited significant anti-inflammatory activity in the *P. acnes*-induced THP-1 cell line with $IC_{50}$ value of 7.96 ± 0.36 μmol/L (retinoic acid as the positive control), and reduced the phosphorylation levels of ERK and p38 in a dose-dependent manner in WWestern blot experience. Herein, we described the isolation, structural identification, and biological evaluation of isolated limonoids.

## 2. Result and discussion

Twenty A/B spiro-type limonoids (Fig. 1) including 7 new limonoids with neotecleanin-type limonoids (**1**–**7**), 7 novel limonoids with 5-oxatricyclo[5.4.0.1[1,4]]hendecane ring system (**8**–**14**), and 2 key precursors (**15**–**16**) along with 4 known limonoids (**17**–**20**) were isolated from the root barks of *Walsura robusta* based on the application of HPLC with DAD detector and preparative HPLC instruments. In this study, the starting point is that the crude extracts of the root barks of *W. robusta* was detected by HPLC with the reference substance cedrelone, 11$\beta$-acetoxycedrelone and 11$\beta$-hydroxycedrelone (Supporting Information Fig. S1) after regular liquid–liquid extraction. Then, the major constituents, including cedrelone, 11$\beta$-acetoxycedrelone and 11$\beta$-

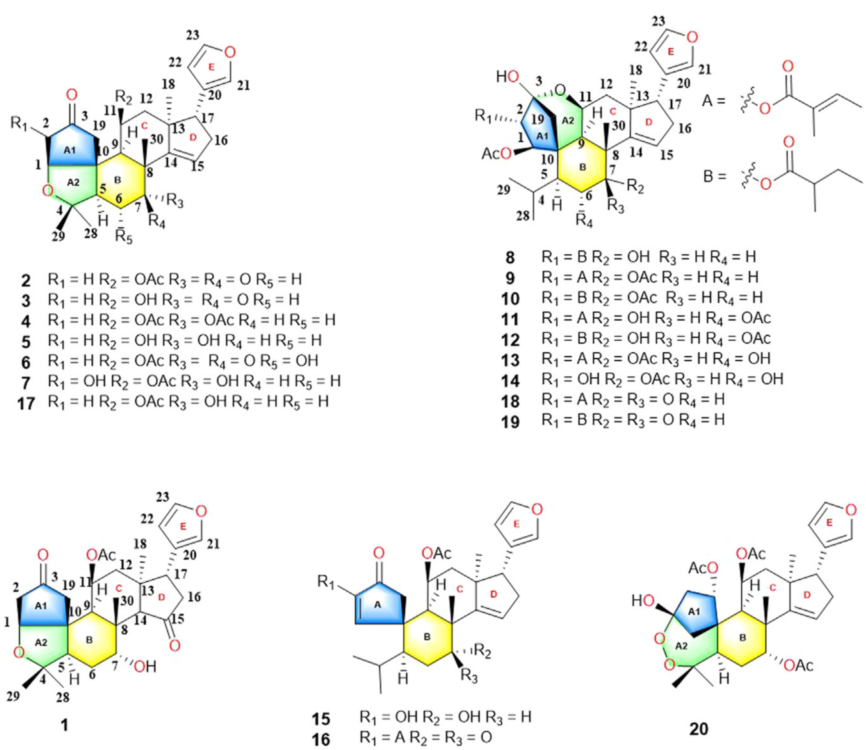


**Figure 1** The structures of compounds **1**–**20**.

hydroxycedrelone, were located and filtered by preparative HPLC instruments with UV detector. Thirdly, the trace fractions of the constituent was enriched and re-verified by HPLC. Subsequently, careful isolation by comprehensive column chromatography followed by HPLC and purified by preparative HPLC afforded analytically pure compounds **1**–**20**. Their structures, including their absolute configurations, were elucidated based on analyses of HR-ESI-MS, 1D/2D NMR, ECD spectrum calculations and single-crystal X-ray diffraction techniques.

Compound **1** was obtained as colorless crystals. The molecular formula of **1** was determined as $C_{28}H_{36}O_7$ based on the positive model HR-ESI-MS ion peak at *m/z* 502.2802 $[M+NH_4]^+$ (Calcd. 502.2799) and $^{13}C$ NMR data, incorporating 11 indices of hydrogen deficiency. The diagnostic 1D NMR data implied the presence of a *β*-substituted furan moiety ($\delta_H$ 7.39, 7.11, 6.15, s, 3H each s; $\delta_C$ 143.5, 139.5, 122.6, 110.5), 2 carbonyl carbons ($\delta_C$ 220.8, 217.5) and an acetyl group ($\delta_H$ 2.09, s; $\delta_C$ 170.1, 21.6), which accounted for 6 out of the 11 indices of hydrogen deficiency. The aforementioned data suggested that **1** is a limonoid possessing a pentacyclic framework similar to walsuranin B[17].

The planar structure of **1** was assigned form its 2D NMR data (Fig. 2). Two carbonyl groups in rings $A_1$ and D were assigned by the HMBC correlations from $H_2$-19 ($\delta_H$ 2.90, d, $J=19.0$ Hz; 2.50, d, $J=19.0$ Hz) and $H_2$-2 ($\delta_H$ 2.42, m; 2.35, dt, $J=18.0$, 3.0 Hz) to C-3 ($\delta_C$ 217.5), and from $H_2$-16 ($\delta_H$ 2.52, d, $J=10.0$) and H-14 ($\delta_H$ 2.88, s) to C-15 ($\delta_C$ 220.8), respectively. The acetyl group was located at C-11 ($\delta_C$ 72.5) based on the HMBC correlation from H-11 ($\delta_H$ 5.20, brd s) to acetyl carbonyl carbon. The located position of *β*-substituted furan moiety was determined at C-17 ($\delta_C$ 38.9) by the HMBC correlations from H-17 ($\delta_H$ 3.76, t, $J=10.0$ Hz) to C-20, C-21 and C-22. The ROESY correlations between H-17, H-12*α* ($\delta_H$ 2.26, dt, $J=16.0$, 2.5 Hz), H-14 and H-11, between Me-30 ($\delta_H$ 1.31, s) and H-7 ($\delta_H$ 3.84, m) indicated that these protons were co-facial and *α*-oriented. The ROESY correlations between H-1, H-5 ($\delta_H$ 2.15, m) and H-9 ($\delta_H$ 1.87, d, $J=2.5$ Hz) suggested that they were *α*-orientation. The ring $A_2$ was speculated as a tetrahydrofuran ring built by the ether bond between C-1 and C-4. However, this speculation could not be confirmed according to the unobserved HMBC correlation from H-1 ($\delta_H$ 4.30, d, $J=3.0$ Hz) to C-4 ($\delta_C$ 81.1). The spectroscopically elucidated structure of **1** was ultimately confirmed though a single-crystal X-ray diffraction study using Cu K*α* radiation [Flack parameter of 0.01], and the absolute configuration of **1** was assigned as 1*S*, 5*R*, 7*R*, 8 *R*, 9*S*, 10*R*, 11*R*, 13*S*, 14*S* and 17*R* (Fig. 3).

Compound **2**, a white amorphous powder, exhibited the molecular formula of $C_{28}H_{34}O_6$ as deduced from the (+)-HR-ESI-MS ion at *m/z* 484.2692 $[M+NH_4]^+$ (Calcd. 484.2694, $C_{28}H_{38}NO_6$) and $^{13}C$ NMR data. Comparison of the 1D and 2D NMR data (Supporting Information Fig. S2) of **1** and **2** showed similarity except for the presence of an additional olefinic hydrogen in $^1H$ NMR data and two additional olefinic carbons in $^{13}C$ NMR. Thus, the afore-mentioned information suggested that they were closely related analogues featuring identical carbon frameworks. The olefinic bond was located as C-14 ($\delta_C$ 150.7) and C-15 ($\delta_C$ 128.3) as reported walrobsin A[10], which was confirmed by the HMBC correlation from H-15 ($\delta_H$ 6.22, brd s) to C-16 ($\delta_C$ 34.7) and C-17 ($\delta_C$ 52.2). The corresponding carbonyl groups were located at C-3 ($\delta_C$ 216.4) and C-7 ($\delta_C$ 207.4) instead of C-3 and C-14. The HMBC correlations from H-5 ($\delta_H$ 2.17, dd, $J=18.5$, 3.5 Hz), $H_2$–6 ($\delta_H$ 2.78, t, $J=15.0$ Hz; 2.44 m) and H-9 ($\delta_H$ 2.55 overlapped) to C-7 confirmed the conclusion, and the structure of **2** were thus determined as depicted. The molecular weight of compound **3** showed 42 Da less than **2** as deduced from the (+)-HR-ESI-MS ion at *m/z* 425.2324 $[M+H]^+$(Calcd. 425.2323, $C_{26}H_{33}O_5$) and $^{13}C$ NMR data of **3**. Comparison of the $^1H$ NMR data (Supporting Information Fig. S3) of **2** and **3** exhibited similarity except for the absence of an acetyl group. Thus, the structure of **3** was determined as 11-deacetyl derivative of **2**.

Compounds **4** and **5**, white amorphous powders, showed that their molecular formulas were $C_{30}H_{38}O_7$ and $C_{26}H_{34}O_5$ deduced from the (+)-HR-ESI-MS ions at *m/z* 528.2957 $[M+NH_4]^+$ and 444.2742 $[M+NH_4]^+$, respectively, and also from their $^{13}C$ NMR data. Comparison of the 1D NMR data of **4** and **5** with those of walsuranin B (**17**)[17] suggested that **4** was a 7-acetyl derivative of **17** and **5** was an 11-deacetyle derivative of **17**, respectively. Analysis of the 1D NMR data and ESI-MS data of **4** and **5** confirmed this deduction by the presence of diagnostic resonances of 2 acetyloxy groups ($\delta_H$ 1.98, 1.97 each 3Hs; $\delta_C$ 170.5, 21.6; 169.8, 21.3) in **4** and the absence of acetyloxy group in **5**. The key HMBC correlation of **4** from H-7 ($\delta_H$ 5.24, t, $J=2.5$ Hz) to an acetyl group ($\delta_C$ 169.8) determined its structure as 7-acetyl derivative of **17** as shown in Fig. 1. Compared to the $^1H$ NMR data of **4**, the absence of two acetyl groups in that of **5** indicated that **5** was an 11-deacetyle derivative of **17**, which was consistent with the HMBC correlations from H-7 ($\delta_H$ 3.96, t, $J=3.0$ Hz) to C-8 ($\delta_C$ 45.9), C-6 ($\delta_C$ 26.4) and from H-11 to C-9 ($\delta_C$ 43.2) and C-12 ($\delta_C$ 45.7).

Compound **6**, a white amorphous powder, displayed a molecular ion at *m/z* 502.2803 $[M+NH_4]^+$ (Calcd. 502.2799) in the (+)-HR-ESI-MS data and determined its molecular formula as $C_{28}H_{36}O_7$ together with $^{13}C$ NMR data. Comparison of the HR-ESI-MS data of **6** and **2** suggested that **6** was 16 Da greater than that of **2** and was identified as the oxidative product of **2**. The $^1H$ NMR and $^{13}C$ NMR spectra of **6** were quite similar to those of

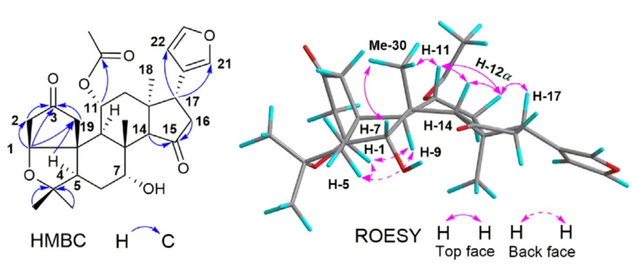


**Figure 2** Selective HMBC and ROESY correlations of compound **1**.

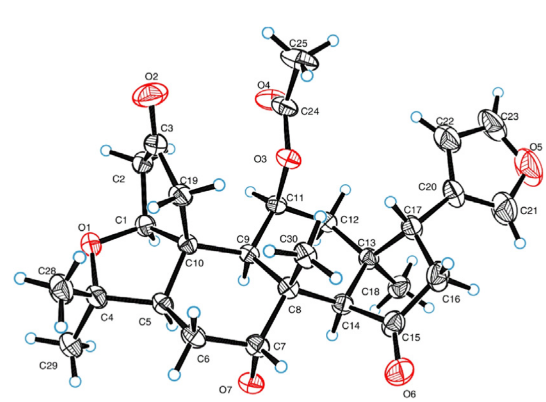

**Figure 3** ORTEP drawing of the compound **1**.

**2** except for the chemical shift of H-6 down shifted from $\delta_H$ 2.47 to 4.07 and the chemical shift of C-6 down shifted from $\delta_C$ 38.2 to 68.4. Thus, compound **6** was deduced as 5-hydroxy derivative of **2**, which was determined by HMBC correlations from H-7 ($\delta_H$ 3.92, brd s), H-5 ($\delta_H$ 2.51, m) to C-6 ($\delta_C$ 68.4). In ROESY spectra, the correlation between H-6 ($\delta_H$ 4.07, m) and H-7, Me-30 ($\delta_H$ 1.39, s), $H_2$-19 ($\delta_H$ 2.96, d, $J=19.0$ Hz; 2.56, $J=19.0$ Hz) suggested the 6-OH and 7-OH were $\beta$-orientation. The structure of **6** was determined as shown and named as walrobsin H.

The $^1$H NMR and $^{13}$C NMR data of **7** were similar to those of walsuranin B (**17**), with the major difference being the chemical shift of H-2 down shifted from $\delta_H$ 2.13 to 3.51 and the chemical shift of C-2 down shifted from $\delta_C$ 45.2 to 58.6. The molecular weight of **7** exhibiting 16 Da greater than that of **17** in ESI-MS data indicated that compound **7** is a 2-oxidation product of **17**. Its molecular formula was determined as $C_{28}H_{36}O_7$ based on a molecular ion at *m/z* 502.2801 $[M+NH_4]^+$ (Calcd. $C_{28}H_{40}NO_7$ 502.2799) in positive HR-ESI-MS spectra. The special A1-A2 ring structure could be determined by the key HMBC correlations of H-1/C-2, C-3, C-19, H-2/C-10, H-19/C-9, C-10, Me-28,29/C-4, C-5, and H-5/C-19. The location of OH was assigned at C-2 based on the key HMBC correlations from H-1 ($\delta_H$ 3.79, d, $J=2.0$ Hz) and $H_2$-19 ($\delta_H$ 2.82, d, $J=19.0$ Hz; $\delta_H$ 2.73, d, $J=19.0$ Hz) to C-2, and from H-2 to C-1 ($\delta_C$ 64.4), C-3 ($\delta_C$ 205.7) and C-19 ($\delta_C$ 37.6). The vicinal coupling constant (2.0 Hz) implied *cis* configuration between H-1 and H-2, which was also determined by the correlations of H-1/H-2, H-1/H-9 and H-2/H-11. Thus, the planar structure and relative configuration of **7** were determined as shown in Fig. 4.

The molecular formula of walrobsin J (**8**), $C_{33}H_{46}O_8$ with 11 degrees of unsaturation, was deduced from its HR-ESI-MS data with a molecular ion at *m/z* 593.3085 $[M+H]^+$ (Calcd. for $C_{33}H_{46}O_8Na$, 593.3085). Similar NMR data indicated that **8** was a limonoid the same as **19**, except for a 2 amu greater than that of **19** in positive model HR-ESI-MS data, as well as the loss of a carbonyl carbon and the appearance of an oxygen carbon ($\delta_C$ 71.4) in $^{13}$C NMR spectrum. Thus, the structure of **8** was determined as shown in Fig. 5, which was elucidated by the key HMBC correlations from H-5 ($\delta_H$ 2.10, m), H-6 ($\delta_H$ 1.68, m) and $H_3$-30 ($\delta_H$ 1.36, s) to C-7 ($\delta_C$ 71.4), and the key ROESY correlation between $H_3$-30 ($\delta_H$ 1.36, s) and H-7 ($\delta_H$ 3.95, s).

The molecular formula of walrobsin K (**9**) and walrobsin L (**10**) as $C_{35}H_{46}O_9$ and $C_{35}H_{48}O_9$, respectively, according to their HR-ESI-MS data *m/z* 611.3212 $[M+H]^+$ (Calcd. for $C_{35}H_{47}O_9$, 611.3215) and *m/z* 613.3370 $[M+H]^+$ (Calcd. for $C_{35}H_{49}O_9$, 613.3372). Compound **10** was determined as the 7$\beta$-acetylate-

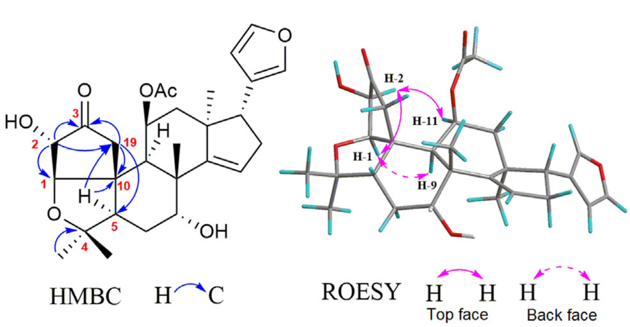


**Figure 4** Selective HMBC and ROESY correlations of **7**.

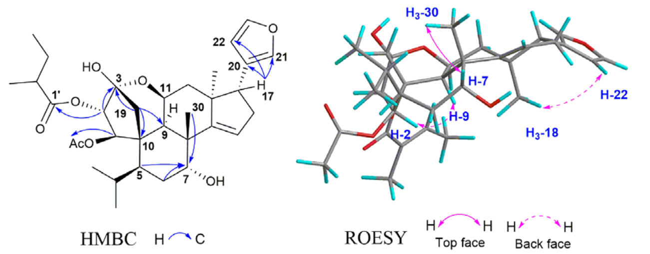


**Figure 5** Selective HMBC and ROESY correlations of **8**.

walrobsin C based on the HMBC correlation from 7-OAc ($\delta_H$ 2.18, s) to C-7 ($\delta_C$ 77.4) and an additional 42 mass unit in HR-ESI-MS data. Walrobsin K (**9**) was subsequently determined as shown in Fig. 2, whose substitutional group at C-1 ($\delta_C$ 86.6) was "A" instead of "B" in **10**.

Walrobsin M (**11**) and walrobsin N (**12**) showed same molecular formulas as **9** and **10**, respectively, according to their HR-ESI-MS data *m/z* 649.2980 $[M+Na]^+$ (Calcd. for $C_{35}H_{46}O_{10}Na$, 649.2983) and *m/z* 651.3138 $[M+Na]^+$ (Calcd. for $C_{35}H_{48}O_{10}Na$, 651.3140). Compound **11** differed form **9** only in the location of OAc, which was confirmed by the key HMBC correlation from OAc to C-6 ($\delta_C$ 72.4) instead of C-7. The configuration of OAc was in $\alpha$ position, which was assigned by the ROESY data between H-6 ($\delta_H$ 5.33, dd, $J=12.0$, 3.0 Hz) and H-4 ($\delta_H$ 2.39, overlapped). The similar condition occurred between **12** and **10**, and its structure was determined as shown in Fig. 1.

The HR-ESI-MS data (*m/z* 627.3166 $[M+Na]^+$; Calcd. for $C_{35}H_{47}O_{10}Na$, 627.3164) showed an additional oxygen atom in the molecular formula of walrobsin O (**13**) compared to **9**. Compound **13** was assigned as 6$\alpha$-*O*-walrobsin K, which was confirmed by the additional oxygen carbon in $^{13}$C NMR data, the further key HMBC correlations from H-4 ($\delta_H$ 1.61, d, $J=12.0$ Hz), H-7 ($\delta_H$ 5.29, d, $J=3.0$ Hz) to C-6 ($\delta_C$ 68.2), and the key ROESY correlation between H-4 and H-6 ($\delta_H$ 4.25, dd, $J=11.5$, 3.0 Hz). Walrobsin P (**14**) differed from **13** in the substituted group at C-1 ($\delta_C$ 91.4), which was confirmed by the disappearance of "A" group in $^1$H NMR and $^{13}$C NMR data, and the loss of 82 amu in its HR-ESI-MS data. Herein, the structures of walrobsins O and P (**13** and **14**) were established as shown in Fig. 1.

Comprehensive analysis of the experimental ECD of type I compounds **1**–**7** and **17** (Supporting Information Fig. S17), allowed the establishment of same absolute configuration of chiral centers as 1*S*, 5*R*, 8*R*, 9*S*, 10*R*, 11*R*, 13*S*, and 17*R*. The assignment of same absolute configuration of chiral centers in type II compounds **8**–**14**, **18** and **19** as 1*R*, 2*S*, 3*R*, 5*S*, 8*R*, 9*R*, 10*S*, 11*S*, 13*S*, and 17*R* using the same method.

Walrobsin Q (**15**), a white amorphous powder, was determined to have a molecular formula of $C_{28}H_{36}O_6$ by the ion at *m/z* 469.2586 $[M+H]^+$ (Calcd. for $C_{28}H_{37}O_6$, 469.2585) in positive model of HR-ESI-MS and $^{13}$C NMR data. Comparison of the $^1$H and $^{13}$C NMR data of **15** with walsuranin C[17], an characteristic isopropyl motif and a furan ring group, suggested that they were structural analogs. Furthermore, one down field shifted proton resonance at $\delta_H$ 3.95 (t, $J=3.0$ Hz, H-7) and one corresponding carbon signal at $\delta_C$ 73.1 were appeared in $^1$H and $^{13}$C NMR spectra, respectively. The above information suggested that the carbonyl group located at C-7 in walsuranin C was reduced as hydroxyl group to form walrobsin Q, which was determined by the HMBC correlations from H-7 to C-6 ($\delta_C$ 37.7), C-8 ($\delta_C$ 52.1) and C-30 ($\delta_C$ 29.0)

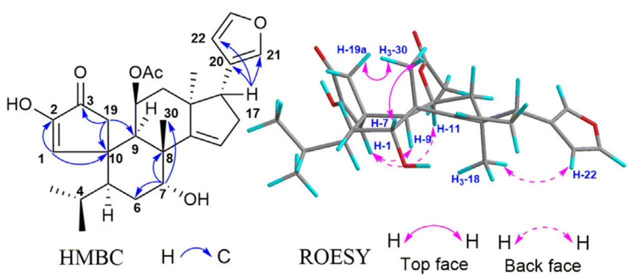


**Figure 6** Selective HMBC and ROESY correlations of **15**.

(Fig. 6). The *penta*-spirocyclic system of A-ring at C-10, and the presence of *α*,*β*-unsaturated carbonyl group in A-ring was similar to walsuranin C validated by the obvious HMBC correlations form H-1 to C-2, C-3, C-10, and from H-19 to C-3, C-9 and C-10. The planar structure of **15** was arbitrarily assigned as in Fig. 6. The similar 1D NMR data indicated that they shared the same relative configuration in skeleton core. The key ROESY correlations of H-1/H-9, H-11, and H-18/H-22 showed that these protons were co-facial and determined as *α*-orientation. The correlations of H-30/H-19a, H-7 were also observed in ROESY spectra and assigned these protons as *β*-orientation. The hydroxyl group were assigned as *α*-oriented by the ROESY correlations H-7/H-30. Compound **16** have a molecular formula of $C_{31}H_{38}O_6$ by the HR-ESI-MS data and $^{13}C$ NMR spectra. Comparison of the $^1H$ and $^{13}C$ NMR data between **16** and walsuranin C[17], the absence of an acetyl group at C-11 and the appearance of an additional tigloyl group ($\delta_H$ 7.16, m; 1.91, s; 1.88, d, $J$=7.0, 1.5 Hz; $\delta_C$ 161.1, 149.8, 127.0, 14.8 12.0) observed in $^1H$ NMR and $^{13}C$ NMR data, which were also consistent with the HR-ESI-MS data (**16**, Calcd. for $C_{31}H_{38}O_6Na$, 529.2561; walsuranin C, $C_{28}H_{34}O_6Na$, 489.2253). Thus, the planar and relative structures of **15** and **16** were determined as shown. Unfortunately, compounds **15** and **16** were not crystallized in aqueous methanol solvent. The absolute configuration of **15** were determined as 1*E*, 5*S*, 7*R*, 8*R*, 9*R*, 10*S*, 11*S*, 13*S*, 14*E* and 17*R* by the well-matched experimental ECD data and the calculated ECD data under time-dependent density functional theory[18] (Fig. 7). The ECD data of **15** and **16** detected in acetonitrile solvent were well matched indicating that they shared the same absolute configuration and that of **16** was assigned as 2′*E*, 1*E*, 5*S*, 8*R*, 9*R*, 10*S*, 11 *S*, 13*S*, 14*E* and 17*R* (Supporting Information Fig. S132). The hypothetical biosynthesis pathway of all isolated compounds was illustrated in Scheme 1. Four types A-ring rearranged limonoids started from cedrelone type limonoids based on comprehensive free radical reaction, oxidation, acylation and hemiketal formation reactions under the help of some enzymes in plant cells (Scheme 1).

In the anti-inflammatory activity evaluation, compounds **1–3**, **8–14**, and **18–20** were tested in three inflammatory models including LPS-induced RAW 264.7, BV2 and *P. acnes*-stimulated THP-1 cell line. Limonoids with 5-oxatricyclo[5.4.0.1[1,4]]hendecane ring system showed better significant anti-inflammatory activity than other A ring rearranged limonoids in this study as shown in Table 5 implying that the hexatomic oxygen heterocycle is essential. Furthermore, compound **11** exhibited significant anti-inflammatory activity in the *P. acnes* induced THP-1 cell line with $IC_{50}$ value 7.96±0.36 μmol/L (retinoic acid as the positive control). In Western blot experience, walrobsin M (**11**) could reduce the phosphorylation levels of ERK and p38 in a dose-dependent manner (Fig. 8). These results reinforced the significance in the discovery of new anti-inflammatory leading-drugs and/or cosmetic ingredients.

## 3. Conclusions

As an illustrative case study, 20 mg level A/B spiro-type limonoids including 7 new neotecleanin-type limonoids (**1–7**), 7 novel limonoids with 5-oxatricyclo[5.4.0.1[1,4]]hendecane ring system (**8–14**), and 2 key precursors (**15–16**) along with four known limonoids (**17–20**) were isolated from the root barks of *W. robusta*. In the anti-inflammatory evaluation, compounds **2**, **8**, **9**, **11**, **13**, **14** and **18** showed significant anti-inflammatory activities in LPS-induced RAW 264.7 cell line, BV2 microglial cells, and *P. acnes*-stimulated THP-1 human monocytic cells. Walrobsin M (**11**) significantly inhibited inflammatory activity with $IC_{50}$ value of 7.96±0.36 μmol/L, and down-regulated phosphorylation levels of ERK and p38 in a dose-dependent manner. Our results further proved a valuable strategy for discovery of trace and/or bioactive compounds.

## 4. Experimental

### 4.1. General experimental procedures

Optical rotations were measured with a JASCO P-1020 polarimeter in solvent MeOH at the sodium D line (589 nm) at 25 °C. The UV spectra were obtained on a UV-2450 UV–Vis spectrophotometer. Nuclear magnetic resonance (NMR) spectra were on a Bruker AVIII-500 NMR spectrometer ($^1H$: 500 MHz, $^{13}C$: 125 MHz) (Bruker, Karlsruhe, Germany), with tetramethylsilane (TMS) as an internal standard. Chemical shift values ($\delta$) are given in parts per million (ppm) and coupling constants in Hertz (Hz). Electrospray ionization (ESI) and high-resolution electrospray ionization (HR-ESI-MS) were carried out an Agilent 1100 series LC/MSD ion trap mass spectrometer and an Agilent 6529B Q-TOF instrument (Agilent Technologies, Santa Clara, CA, USA), respectively. HPLC analyses were performed using an Agilent 1260 system equipped with a RP-C18 column (250 mm × 4.6 mm, 5 μm, Agilent, Santa Clara, CA, USA). Preparative high-performance liquid chromatography (Pre-HPLC) was performed on a Shimadzu LC-8A system equipped with a Shim-pack RP-C18 column (200 mm × 20 mm i.d., 10 μm, Shimadzu, Tokyo, Japan) detected by a binary channel UV detector at 210 and 230 nm. The parameters of flow rate and column temperature were set as 10.0 mL/min and 25 °C , respectively. All solvents used were of analytical grade. Silica gel (200–300 mesh; Qingdao Haiyang Chemical Co., Ltd., Qingdao, China), MCI (Mitsubishi, Tokyo, Japan) and YMC RP-C18 silica (40–63 μm; Milford, MA, USA) were used for column chromatography. Fractions obtained from repetitive column chromatography (CC) were monitored by thin-layer chromatography (TLC) with precoated silica gel $GF_{254}$ plates (Qingdao Haiyang Chemical Co., Ltd., Qingdao, China). Spots were observed under UV lamp at 254 and/or 365 nm, and then visualized by heating silica gel plates sprayed with vanillin-sulfuric acid.

### 4.2. Plant material

Air-dried root barks of *W. robusta*, which were deposited in the Department of Natural Medicinal Chemistry, China Pharmaceutical University (China, accession number 2015-GSS), were collected from Xishuangbanna, China, in September 2015, and were authenticated by Professor Shuncheng Zhang, Xishuangbanna Tropical Botanical Garden, Chinese Academy of Sciences, China.

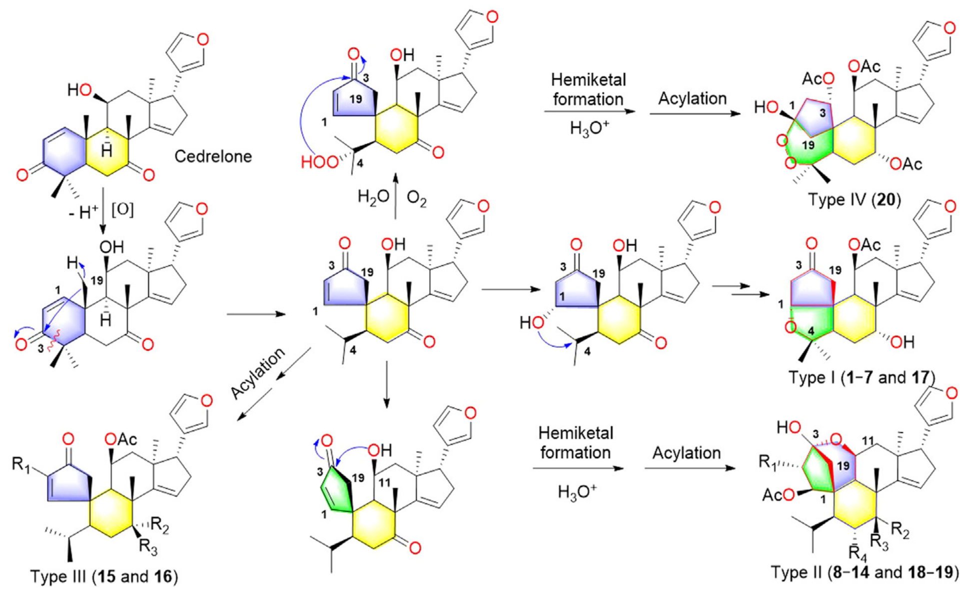


**Scheme 1** Hypothetical biosynthetic pathways of four types A-ring rearranged limonoids **1**–**20**.

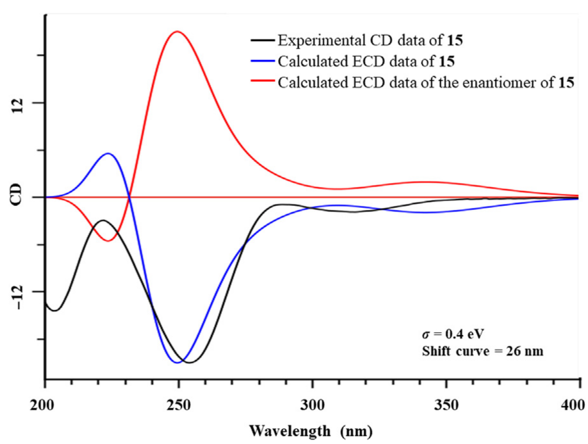


**Figure 7** Experimental ECD spectra of compound **15** overlaid with the calculated ECD spectra of **15** and its enantiomers.

### 4.3. *Extraction and isolation*

The dried powder of fruits of *W. robusta* (5.0 kg) was extracted three times (3 × 5 L) with 95% EtOH–$H_2O$ under reflux, and the crude (500 g) was suspended in $H_2O$ and extracted with petroleum ether (PE) (3 times with 1 L each) and EtOAc (3 times with 1 L each), successively. The EtOAc extract (100.0 g) was chromatographed on a silica gel column (100 mush, 300 g), eluted with a gradient of $CH_2Cl_2$–MeOH (100:1, 50:1, 25:1, 10:1 and 5:1, *v/v*) to give six fractions (A–F), which were combined based on TLC (vanillin-sulfuric acid as color-developing agent). Medium polarity fraction E (≈ 10.0 g) was chromatographed over a middle chromatogram isolated (MCI) column eluted with a gradient system of MeOH–H2O (50:5, 75:25 and 95:5, *v/v*) to afford three subfractions (EA–EC), respectively. EB fraction (≈ 4.5 g) was sequentially purified by columns of RP-C18 silica gel (MeOH–$H_2O$, 50%–75%, *v/v*) and then further separated over semi-preparative HPLC to "filter" the major and "impurity" ingredients including cedrelone, 11*β*-acetoxycedrelone and 11*β*-hydroxycedrelone, with walrobsins A (**18**) and B (**19**) as "light" target as shown in Fig. 1. Finally, 20 new compounds (**1**–**16**) and 4 known compounds (**17**–**20**) were obtained from the "filtered" extracts. Walrobsins C-R (**1**–**16**) and known compounds (**17**–**20**) were yielded as **1** (5 mg), **2** (20 mg), **3** (7 mg), **4** (4 mg), **5** (5 mg), **6** (4 mg), **7** (10 mg), **8** (3 mg), **9** (10 mg), **10** (14 mg), **11** (20 mg), **12** (30 mg), **13** (5 mg), **14** (5 mg), **15** (4 mg), **16** (2 mg), **17** (30 mg), **18** (40 mg), **19** (35 mg) and **20** (14 mg), respectively (detailed procedure for extraction and isolation, see Supporting Information).

#### 4.3.1. *Walrobsin C (**1**)*

Colorless crystals; $[\alpha]_D^{23}$ –18.6 (*c* 0.139, MeOH); UV (MeOH) $\lambda_{max}$ (log*ε*) 210 (4.07) nm; IR $\nu_{max}$ 3435, 2965, 1727, 1378, 1233, 1171, 1042, 873, 790, 602 $cm^{-1}$; $^1H$ and $^{13}C$ NMR ($CDCl_3$), see Tables 1 and 4; negative ESI-MS *m/z* 519.18 $[M+Cl]^-$; positive ESI-MS *m/z* 502.24 $[M+NH_4]^+$; HR-ESI-MS *m/z* 502.2802 $[M+NH_4]^+$ (Calcd. for $C_{28}H_{40}NO_7$, 502.2799).

#### 4.3.2. *Walrobsin D (**2**)*

White powder; $[\alpha]_D^{23}$ –54.2 (*c* 0.197, MeOH); UV (MeOH) $\lambda_{max}$ (log*ε*) 209 (4.72) nm; IR $\nu_{max}$ 3234, 2970, 2933, 1742, 1638, 1453, 1381, 1236, 1012, 820, 609 $cm^{-1}$; $^1H$ and $^{13}C$ NMR ($CDCl_3$), see Tables 1 and 4; negative ESI-MS *m/z* 501.28 $[M+Cl]^-$; positive ESI-MS *m/z* 484.28 $[M+NH_4]^+$; HR-ESI-MS *m/z* 484.2692 $[M+NH_4]^+$ (Calcd. for $C_{28}H_{38}NO_6$, 484.2694).

#### 4.3.3. *Walrobsin E (**3**)*

White powder; $[\alpha]_D^{23}$ –81.3 (*c* 0.174, MeOH); UV (MeOH) $\lambda_{max}$ (log*ε*) 208 (4.63) nm; IR $\nu_{max}$ 3429, 2933, 1741, 1454, 1383, 1196, 1157, 1011, 823, 602 $cm^{-1}$; $^1H$ and $^{13}C$ NMR ($CDCl_3$), see Tables 1 and 4; negative ESI-MS *m/z* 459.10 $[M+Cl]^-$; positive ESI-MS *m/z* 425.21 $[M+H]^+$; HR-ESI-MS *m/z* 425.2324 $[M+H]^+$ (Calcd. for $C_{26}H_{33}O_5$, 425.2323).

#### 4.3.4. *Walrobsin F (**4**)*

White powder; $[\alpha]_D^{23}$ –22.7 (*c* 0.165, MeOH); UV (MeOH) $\lambda_{max}$ (log*ε*) 208 (4.69) nm; IR $\nu_{max}$ 3436, 2930, 1741, 1375, 1236, 1030, 943, 873, 601 $cm^{-1}$; $^{1}H$ and $^{13}C$ NMR ($CDCl_3$), see Tables 1 and 4; negative ESI-MS *m/z* 545.24 $[M+Cl]^-$; positive ESI-MS *m/z* 528.25 $[M+NH_4]^+$; HR-ESI-MS *m/z* 528.2957 $[M+NH_4]^+$ (Calcd. for $C_{30}H_{42}NO_7$, 528.2956).

#### 4.3.5. Walrobsin G (5)

White powder; $[\alpha]_D^{23}$ –68.4 (*c* 0.371, MeOH); UV (MeOH) $\lambda_{max}$ (log$\varepsilon$) 215 (4.43) nm; IR $\nu_{max}$ 3434, 2926, 1736, 1456, 1381, 1113, 1038, 1000, 874 $cm^{-1}$; $^{1}H$ and $^{13}C$ NMR ($CDCl_3$), see Tables 1 and 4; negative ESI-MS *m/z* 461.21 $[M+Cl]^-$; positive ESI-MS *m/z* 444.23 $[M+NH_4]^+$; HR-ESI-MS *m/z* 444.2742 $[M+NH_4]^+$ (Calcd. for $C_{26}H_{38}NO_5$, 444.2744).

#### 4.3.6. Walrobsin H (6)

White powder; $[\alpha]_D^{23}$ –9.0 (*c* 0.126, MeOH); UV (MeOH) $\lambda_{max}$ (log$\varepsilon$) 207 (4.70) nm; IR $\nu_{max}$ 3436, 2931, 1740, 1382, 1238, 1079, 1028, 1002, 873, 601 $cm^{-1}$; $^{1}H$ and $^{13}C$ NMR ($CDCl_3$), see Tables 1 and 4; negative ESI-MS *m/z* 519.21 $[M+Cl]^-$; positive ESI-MS *m/z* 502.25 $[M+NH_4]^+$; HR-ESI-MS *m/z* 502.2803 $[M+NH_4]^+$ (Calcd. for $C_{28}H_{40}NO_7$, 502.2799).

#### 4.3.7. Walrobsin I (7)

White powder; $[\alpha]_D^{23}$ –22.7 (*c* 1.10, MeOH); UV (MeOH) $\lambda_{max}$ (log$\varepsilon$) 221 (4.13) nm; IR $\nu_{max}$ 3467, 2936, 1740, 1456, 1381, 1237, 1159, 1035, 1001, 873, 819, 773, 601 $cm^{-1}$; $^{1}H$ and $^{13}C$ NMR ($CDCl_3$), see Tables 1 and 4; negative ESI-MS *m/z* 519.23 $[M+Cl]^-$; positive ESI-MS *m/z* 507.26 $[M+Na]^+$; HR-ESI-MS *m/z* 502.2801 $[M+NH_4]^+$ (Calcd. for $C_{28}H_{40}NO_7$, 502.2799).

#### 4.3.8. Walrobsin J (8)

White powder; $[\alpha]_D^{23}$ –0.6 (*c* 0.204, MeOH); UV (MeOH) $\lambda_{max}$ (log$\varepsilon$) 209 (4.68) nm; IR $\nu_{max}$ 3436, 2968, 1744, 1461, 1384, 1304, 1229, 1063, 1031, 874, 602 $cm^{-1}$; $^{1}H$ and $^{13}C$ NMR ($CDCl_3$), see Tables 2 and 4; negative ESI-MS *m/z* 605.37 $[M+Cl]^-$; positive ESI-MS *m/z* 588.31 $[M+NH_4]^+$; HR-ESI-MS *m/z* 593.3086 $[M+Na]^+$ (Calcd. for $C_{33}H_{46}NaO_8$, 593.30859).

#### 4.3.9. Walrobsin K (9)

White powder; $[\alpha]_D^{23}$ –7.9 (*c* 0.211, MeOH); UV (MeOH) $\lambda_{max}$ (log$\varepsilon$) 216 (4.86) nm; IR $\nu_{max}$ 3434, 2966, 1743, 1370, 1253, 1161, 1029, 733, 605 $cm^{-1}$; $^{1}H$ and $^{13}C$ NMR ($CDCl_3$), see Tables 2 and 4; negative ESI-MS *m/z* 645.17 $[M+Cl]^-$; positive ESI-MS *m/z* 628.21 $[M+NH_4]^+$; HR-ESI-MS *m/z* 611.3212 $[M+H]^+$ (Calcd. for $C_{35}H_{47}O_9$, 611.3215).

#### 4.3.10. Walrobsin L (10)

White powder; $[\alpha]_D^{23}$ –1.9 (*c* 0.208, MeOH); UV (MeOH) $\lambda_{max}$ (log$\varepsilon$) 208 (4.68) nm; IR $\nu_{max}$ 3412, 2965, 1750, 1711, 1458, 1260, 1225, 1035, 873, 605 $cm^{-1}$; $^{1}H$ and $^{13}C$ NMR ($CDCl_3$), see Tables 2 and 4; negative ESI-MS *m/z* 611.27 $[M-H]^-$; positive ESI-MS *m/z* 635.36 $[M+Na]^+$; HR-ESI-MS *m/z* 635.3190 $[M+Na]^+$ (Calcd. for $C_{35}H_{48}O_9Na$, 635.3191).

#### 4.3.11. Walrobsin M (11)

White powder; $[\alpha]_D^{23}$ +39.4 (*c* 0.208, MeOH); UV (MeOH) $\lambda_{max}$ (log$\varepsilon$) 215 (4.87), 277 (3.79) nm; IR $\nu_{max}$ 3436, 2934, 1722, 1370, 1252, 1163, 1030, 874, 736, 601 $cm^{-1}$; $^{1}H$ and $^{13}C$ NMR ($CDCl_3$), see Tables 2 and 4; negative ESI-MS *m/z* 625.31 $[M-H]^-$, 661.30 $[M+Cl]^-$; positive ESI-MS *m/z* 644.26 $[M+NH_4]^+$; HR-ESI-MS *m/z* 649.2980 $[M+Na]^+$ (Calcd. for $C_{35}H_{46}O_{10}Na$, 649.2983).

#### 4.3.12. Walrobsin N (12)

White powder; $[\alpha]_D^{23}$ +61.4 (*c* 0.158, MeOH); UV (MeOH) $\lambda_{max}$ (log$\varepsilon$) 207 (4.75) nm; IR $\nu_{max}$ 3444, 2935, 1742, 1461, 1370, 1229, 1163, 1030, 874, 799, 601 $cm^{-1}$; $^{1}H$ and $^{13}C$ NMR ($CDCl_3$), see Tables 2 and 4; negative ESI-MS *m/z* 663.11 $[M+Cl]^-$; positive ESI-MS *m/z* 629.16 $[M+H]^+$; HR-ESI-MS *m/z* 651.3138 $[M+Na]^+$ (Calcd. for $C_{35}H_{48}O_{10}Na$, 651.3140).

#### 4.3.13. Walrobsin O (13)

White powder; $[\alpha]_D^{23}$ +48.1 (*c* 0.201, MeOH); UV (MeOH) $\lambda_{max}$ (log$\varepsilon$) 212 (4.85) nm; IR $\nu_{max}$ 3446, 2934, 2360, 1741, 1373, 1254, 1163, 1030, 874, 733, 601 $cm^{-1}$; $^{1}H$ and $^{13}C$ NMR ($CDCl_3$), see Tables 2 and 4; negative ESI-MS *m/z* 661.25 $[M+Cl]^-$; positive ESI-MS *m/z* 644.29 $[M+NH_4]^+$; HR-ESI-MS *m/z* 627.3166 $[M+H]^+$ (Calcd. for $C_{35}H_{47}O_{10}$, 627.3164).

#### 4.3.14. Walrobsin P (14)

White powder; $[\alpha]_D^{23}$ +55.3 (*c* 0.210, MeOH); UV (MeOH) $\lambda_{max}$ (log$\varepsilon$) 208 (4.64) 270 (3.70) nm; IR $\nu_{max}$ 3435, 2935, 1722, 1371, 1248, 1161, 1026, 874, 798, 736, 601 $cm^{-1}$; $^{1}H$ and $^{13}C$ NMR ($CDCl_3$), see Tables 2 and 4; negative ESI-MS *m/z* 579.21 $[M+Cl]^-$; positive ESI-MS *m/z* 562.28 $[M+NH_4]^+$; HR-ESI-MS *m/z* 545.2744 $[M+H]^+$ (Calcd. for $C_{30}H_{41}O_9$, 545.2745).

#### 4.3.15. Walrobsin Q (15)

White powder; $[\alpha]_D^{23}$ –55.8 (*c* 0.575, MeOH); UV (MeOH) $\lambda_{max}$ (log$\varepsilon$) 215 (4.43), 257 (4.44) nm; IR $\nu_{max}$ 3435, 2957, 1705, 1386, 1242, 1028, 874, 786, 600 $cm^{-1}$; $^{1}H$ and $^{13}C$ NMR ($CDCl_3$), see Tables 3 and 4; negative ESI-MS *m/z* 503.16 $[M+Cl]^-$; positive ESI-MS *m/z* 486.26 $[M+NH_4]^+$; HR-ESI-MS *m/z* 469.2586 $[M+H]^+$ (Calcd. for $C_{28}H_{37}O_6$, 469.2585).

#### 4.3.16. Walrobsin R (16)

White powder; $[\alpha]_D^{23}$ –35.8 (*c* 0.053, MeOH); UV (MeOH) $\lambda_{max}$ (log$\varepsilon$) 212 (4.27), 257 (4.34) nm; IR $\nu_{max}$ 3419, 2931, 2310, 1715, 1646, 1454, 1384, 1253, 1114, 1022, 951, 723, 615 $cm^{-1}$; $^{1}H$ and $^{13}C$ NMR ($CDCl_3$), see Tables 3 and 4; negative ESI-MS *m/z* 547.31 $[M+Cl]^-$; positive ESI-MS *m/z* 524.29 $[M+NH_4]^+$; HR-ESI-MS *m/z* 529.2559 $[M+Na]^+$ (Calcd. for $C_{31}H_{38}O_6Na$, 529.2561).

### 4.4. NO production bioassay

The RAW264.7 cell line and BV-2 cell line were purchased from the Chinese Academic of Sciences. The cells were cultured in DMEM containing 10% FBS with penicillin (100 U/mL) and streptomycin (100 U/mL) at 37 °C in a humidified atmosphere with 5% $CO_2$. The cells were allowed to grow in 96-well plates with $1 \times 10^5$ cells/well to treat test compounds. After being incubated for 2 h, the cells were treated with 100 ng/mL of LPS for 18 h. Nitrite in culture media was measured to assess NO production using Griess reagent. The absorbance at 540 nm was measured on a microplate reader. *N*-monomethyl-L-arginine was used as the positive control. Cytotoxicity was determined by the MTT method after 48 h incubation with test compounds. All the experiments were performed in three independent replicates[19].

### 4.5. Anti-bacterial test

The anti-bacterial activity of selected walrobsins **1–3**, **8–14**, and **19–20** were carried out using a broth microdilution method and the minimum inhibitory concentration (MIC) was determined. *P. acnes* at

**Table 1** [1]H NMR spectroscopic data ($\delta$) for compounds **1**–**7**[a] ($\delta$ in ppm, $J$ in Hz).

| No. | **1** | **2** | **3** | **4** | **5** | **6** | **7** |
|---|---|---|---|---|---|---|---|
| 1 | 4.30 d (3.0) | 4.33 d (3.5) | 4.36 brd s | 4.32 d (3.0) | 4.34 brd s | 4.31 d (3.0) | 3.79 d (2.0) |
| 2a | 2.42 m | 2.44 (overlapped) | 2.78 d (18.0) | 2.33 (overlapped) | 2.71 dd (17.5, 3.0) | 2.37 d (18.5) | 3.51 d (2.0) |
| 2b | 2.35 dt (18.0,3.0) | 2.23 dd (18.5, 3.5) | 2.45 (overlapped) | 2.16 dd (18.0, 3.0) | 2.35 (overlapped) | 2.10 dt (18.5, 3.0) | |
| 5 | 2.51 m | 2.17 dd (16.0, 3.0) | 2.16 dd (15.5 3.0) | 2.33 dd (13.5, 3.0) | 2.52 (overlapped) | 2.51 m | 2.39 dd (13.0, 2.0) |
| 6a | 1.91 dt (13.0, 2.0) | 2.78 t (15.0) | 2.80 dd (15.5, 14.0) | 1.89 td (14.0, 2.5) | 1.85 (overlapped) | 4.07 m | 2.05 m |
| 6b | 1.60 m | 2.44 (overlapped) | 2.47 (overlapped) | 1.78 dd (14.0, 3.0) | | | 1.65 m |
| 7 | 3.84 m | | | 5.24 t (2.5) | 3.96 t (3.0) | 3.92 brd s | 3.89 m |
| 9 | 1.87 d (2.5) | 2.55 (overlapped) | 2.31 d (5.5) | 2.53 d (5.5) | 2.38 d (5.5) | 2.46 d (5.5) | 2.58 d (6.5) |
| 11 | 5.20 brd s | 5.14 dt (9.0, 5.5) | 4.34 dt (9.0, 5.5) | 5.16 dt (9.0, 5.5) | 4.34 (overlapped) | 5.13 td (9.0, 6.0) | 5.42 td (10.0, 5.0) |
| 12a | 2.26 dt (16.0, 2.5) | 2.73 dd (14.0, 10.0) | 2.50 (overlapped) | 2.80 dd (14.0, 9.5) | 2.48 (overlapped) | 2.80 dt (14.0, 9.5) | 2.79 dd (14.0, 9.0) |
| 12b | 1.45 dt (16.0, 4.0) | 1.37 dd (14.0, 5.5) | 1.58 dd (13.0, 7.0) | 1.35 dd (14.0, 5.5) | 1.53 dd (13.0, 7.0) | 1.32 dt (16.0, 6.0) | 1.28 (overlapped) |
| 15 | 2.88 s (H-14) | 6.22 brd s | 6.24 t (2.5) | 5.53 t (2.5) | 5.71 t (2.5) | 5.70 brd d (3.0) | 5.69 brd d (3.0) |
| 16a | 2.52 d (10.0) | 2.55 (overlapped) | 2.57 dd (15.5, 2.0) | 2.42 (overlapped) | 2.57 ddd (16.0,11.0, 2.0) | 2.58 (overlapped) | 2.55 ddd (11.0, 9.5, 2.0) |
| 16b | | 2.44 (overlapped) | 2.47 (overlapped) | | 2.50 (overlapped) | 2.51 (overlapped) | 2.47 ddd (15.5, 7.5, 3.5) |
| 17 | 3.76 t (10.0) | 2.84 dd (11.0, 7.5) | 2.89 dd (11.0, 7.0) | 2.83 dd (11.0, 7.0) | 2.92 dd (11.0, 7.0) | 2.89 dd (11.0, 7.0) | 2.87 dd (11.0,7.0) |
| 18 | 0.76 s | 0.80 s | 0.80 s | 0.82 s | 0.82 s | 0.84 s | 0.83 s |
| 19a | 2.90 d (19.0) | 3.15 d (19.0) | 3.36 d (19.0) | 3.03 d (19.0) | 3.13 d (19.0) | 2.96 d (19.0) | 2.82 d (19.0) |
| 19b | 2.50 d (19.0) | 2.64 d (19.0) | 2.55 d (19.0) | 2.46 d (19.0) | 2.33 d (19.0) | 2.56 d (19.0) | 2.73 d (19.0) |
| 21 | 7.11 s | 7.24 s | 7.27 s | 7.24 s | 7.28 s | 7.25 s | 7.25 s |
| 22 | 6.15 s | 6.23 s | 6.28 s | 6.26 s | 6.28 s | 6.26 s | 6.25 s |
| 23 | 7.39 s | 7.36 s | 7.39 s | 7.37 s | 7.40 s | 7.39 s | 7.38 s |
| 28 | 1.27 s | 1.18 s | 1.26 s | 1.23 s | 1.28 s | 1.37 s | 1.36 s |
| 29 | 1.12 s | 1.26 s | 1.18 s | 1.13 s | 1.14 s | 1.37 s | 1.28 s |
| 30 | 1.31 s | 1.55 s | 1.60 s | 1.40 s | 1.35 s | 1.39 s | 1.43 s |
| 11-OAc | 2.09 s | 1.99 s | | 1.98 s | | 1.96 s | 2.00 s |
| 7-OAc | | | | 1.97 s | | | |

[a]NMR data ($\delta$) were measured at 500 MHz in $CDCl_3$ for **1**–**7**.

**Table 2** [1]H NMR spectroscopic data ($\delta$) for compounds **8–14**[a] ($\delta$ in ppm, $J$ in Hz).

| No. | **8** | **9** | **10** | **11** | **12** | **13** | **14** |
|---|---|---|---|---|---|---|---|
| 1 | 5.16 t (3.0) | 5.31 t (3.0) | 5.11 t (3.0) | 5.23 brd s | 4.80 d (3.5) | 5.21 t (3.0) | 4.47 brd s |
| 2 | 4.80 d (3.5) | 4.90 d (3.5) | 4.83 d (3.5) | 4.80 d (3.5) | 5.17 t (3.0) | 4.82 d (3.0) | 3.83 d (3.5) |
| 4 | 2.44 (overlapped) | 2.50 m | 2.44 m | 2.39 (overlapped) | 2.42 m | | 2.29 m |
| 5 | 2.10 m | 2.51 m | 2.10 m | 2.10 (overlapped) | 2.10 (overlapped) | 1.61 d (12.0) | 2.17 d (12.0) |
| 6a | 1.78 m | 2.51 m | 2.50 m | 5.30 dd (12.0, 3.0) | 4.08 d (3.0) | 4.25 dd (11.5, 3.0) | 5.29 dd (12.0, 2.0) |
| 6b | | 2.37 m | 1.60 m | | | | |
| 7 | 3.95 s | 5.27 d (3.5) | 5.20 d (3.5) | 4.07 d (3.0) | 5.31 dd (12.0, 3.0) | 5.29 d (3.0) | 4.09 d (3.0) |
| 9 | 2.12 (overlapped) | 2.18 m | 2.10 m | 2.23 d (5.5) | | 2.10 d (6.5) | 2.10 d (6.5) |
| 11 | 5.14 td (8.5, 6.0) | 4.52 dt (7.5, 7.0) | 4.46 td (7.5, 7.0) | 4.47 td ( 8.5. 6.0) | 2.23 d ( 6.5) | 4.46 td (8.5, 6.0) | 4.57 td (8.5, 6.0) |
| 12a | 2.86 dd (12.5, 6.5) | 2.33 m | 2.28 dd (12.5, 8.5) | 2.29 dd (13.0, 9.0) | 2.28 dd (13.0, 9.0) | 2.31 (overlapped) | 2.41 m |
| 12b | 1.37 dd (14.0, 5.5) | 1.72 m | 1.65 m | 1.64 dd (13.0, 9.0) | 1.69 (overlapped) | 1.62 (overlapped) | 1.65 dd (13.0,9.0) |
| 15 | 5.63 brd (3.5) | 5.50 brd s | 5.45 brd s | 5.59 t (2.5) | 5.60 t (3.0) | 5.49 brd s | 5.59 brd d (3.0) |
| 16a | 2.60 dd (15.5 11.0) | 2.22 dd (12.5, 2.5) | 2.35 ddd (15.0, 7.0, 3.5) | 2.58 ddd (16.0,11.0, 2.0) | 2.59 ddd (16.0,11.0, 2.0) | 2.36 dd (16.0, 12.0) | 2.57 ddd (15.0,11.0, 2.0) |
| 16b | 2.38 (overlapped) | 1.73 m | 1.63 m | 2.40 (overlapped) | 2.45 (overlapped) | 2.31 (overlapped) | 2.44 (overlapped) |
| 17 | 2.92 dd (11.0, 7.0) | 2.93 dd (11.0, 7.5) | 2.88 dd (11.0, 7.5) | 2.91 dd (11.0, 7.0) | 2.92 dd (11.0, 7.0) | 2.85 dd (11.0, 7.0) | 2.91 dd (11.0 7.0) |
| 18 | 0.76 s | 0.79 s | 0.74 s | 0.76 s | 0.76 s | 0.74 s | 0.72 s |
| 19a | 2.01 (overlapped) | 2.22 m | 2.10 m | 2.17 d (12.5) | 2.17 d (12.5) | 2.18 d (12.5) | 2.01 d (12.5) |
| 19b | 1.81 (overlapped) | 1.73 m | 1.64 m | 2.12 (overlapped) | 2.12 d (12.5) | 2.05 d (12.5) | 1.94 d (12.5) |
| 21 | 7.26, s | 7.29 s | 7.25 s | 7.25 s | 7.26 s | 7.25 s | 7.25 s |
| 22 | 6.27, s | 6.33 s | 6.27 s | 6.28 s | 6.27 s | 6.38 s | 6.28 s |
| 23 | 7.39, s | 7.43 s | 7.38 s | 7.38 s | 7.39 s | 7.38 s | 7.37 s |
| 28 | 0.83 d (7.0) | 0.94 d (7.0) | 0.93 d (7.0) | 1.08 d (7.0) | 1.09 d (7.0) | 1.12 d (7.0) | 1.13 d (7.0) |
| 29 | 0.95 d (7.0) | 0.88 d (7.0) | 0.82 d (7.0) | 0.82 d (7.0) | 0.83 d (7.0) | 1.00 d (7.0) | 0.82 d (7.0) |
| 30 | 1.36 s | 1.44 s | 1.39 s | 1.42 s | 1.42 s | 1.40 s | 1.44 s |
| 2′ | 2.52 (overlapped) | | 1.60 m | | 2.50 m | | |
| 3′ | 1.70 (m) | 7.01 m | 2.50 m | 6.96 m | 1.67 m | 6.96 m | |
| | 1.50 (m) | | 1.60 m | | 1.51 m | | |
| 4′ | 0.92 t (7.0) | 1.89 s | 0.93 t (7.0) | 1.83 s | 0.92 t (7.0) | 1.83 s | |
| 5′ | 1.17 d (7.0) | 1.88 d (6.0) | 1.19 d (7.0) | 1.80 d (6.0) | 1.18 d (7.0) | 1.82 d (6.0) | |
| 7-OAc | 2.10 s | 2.18 s | | 2.12 s (6-OAc) | 2.13 s (6-OAc) | 2.16 s | 2.15 s |
| 11-OAc | | 2.02 s | | 2,12 s | 2,13 s | 2.04 s | 2.13 s |
| OH | | 5.94 s | 5.54 s | | | 5.91 s | |

[a]NMR data ($\delta$) were measured at 500 MHz in $CDCl_3$ for **8–14**.

**Table 3** $^{1}H$ NMR spectroscopic data (δ) for compounds **15** and **16**[a] (δ in ppm, *J* in Hz).

| No. | **15** | **16** | No. | **15** | **16** |
|---|---|---|---|---|---|
| 1 | 6.24 s | 6.27 s | 19 | 3.06 d (19.0), 2.35 d (19.0) | 3.64 d (19.0), 2.60 d (19.0) |
| 4 | 1.48 m | 1.72 m | 21 | 7.24 s | 7.26 s |
| 5 | 1.90 (overlapped) | 2.48 m | 22 | 6.26 s | 7.28 s |
| 6a | 1.91 m | 2.73 t (14.5) | 23 | 7.37 s | 7.38 s |
| 6b | 1.67 m | 2.44 m | | | |
| 7 | 3.95 t (3.0) | | 28 | 0.87 d (7.0) | 0.90 d (7.0) |
| 9 | 2.68 d (6.5) | 2.20 d (4.5) | 29 | 0.80 d (7.0) | 0.86 d (7.0) |
| 11 | 4.57 td (9.0, 6.0) | 4.34 m | 30 | 1.32 s | 1.63 s |
| 12a | 2.67 dd (13.5, 9.0) | 2.80 dd (14.0, 8.5) | 3′ | | 7.16 m |
| 12b | 1.33 (overlapped) | 1.69 dd (13.5, 6.5) | | | |
| 15 | 5.69 brd d (3.0) | 6.28 brd s | 4′ | | 1.91 s |
| 16a | 2.55 ddd (15.5, 11.0, 2.0) | 2.58 (overlapped) | 5′ | | 1.88 dd (7.0,1.5) |
| 16b | 2.48 ddd (15.5, 7.0, 3.0) | 2.42 (overlapped) | | | |
| 17 | 2.87 dd (11.0, 7.5) | 2.92 dd (11.0,7.0) | OAc | 1.90 s | |
| 18 | 0.81 s | 0.86 s | | | |

[a]NMR data (δ) were measured at 500 MHz in $CDCl_3$ for **15** and **16**.

**Table 4** $^{13}C$ NMR spectroscopic data (δ) for compounds **1**–**16**[a] (δ in ppm).

| No. | **1** | **2** | **3** | **4** | **5** | **6** | **7** | **8** | **9** | **10** | **11** | **12** | **13** | **14** | **15** | **16** |
|---|---|---|---|---|---|---|---|---|---|---|---|---|---|---|---|---|
| 1 | 84.4 | 84.1 | 84.4 | 84.6 | 84.8 | 84.5 | 64.4 | 86.4 | 86.6 | 86.4 | 86.0 | 86.2 | 86.1 | 91.4 | 137.0 | 153.0 |
| 2 | 45.5 | 45.1 | 45.8 | 45.4 | 46.3 | 44.7 | 58.6 | 86.1 | 86.3 | 86.3 | 86.5 | 86.0 | 86.6 | 83.3 | 151.9 | 150.5 |
| 3 | 217.5 | 216.4 | 217.3 | 217.5 | 219.1 | 217.5 | 205.7 | 102.1 | 102.0 | 102.1 | 102.0 | 102.1 | 102.1 | 102.4 | 204.6 | 201.3 |
| 4 | 81.1 | 80.7 | 80.6 | 80.8 | 80.9 | 81.3 | 73.7 | 27.3 | 27.3 | 27.3 | 28.2 | 28.1 | 28.1 | 28.2 | 25.4 | 26.6 |
| 5 | 52.6 | 59.5 | 59.6 | 54.6 | 52.9 | 58.0 | 48.3 | 37.1 | 38.2 | 39.1 | 41.1 | 41.1 | 45.0 | 41.2 | 44.2 | 51.7 |
| 6 | 27.7 | 38.1 | 38.2 | 26.1 | 26.4 | 68.4 | 29.3 | 24.3 | 23.6 | 23.6 | 72.4 | 72.6 | 68.2 | 72.7 | 27.0 | 37.7 |
| 7 | 71.3 | 207.4 | 208.1 | 75.9 | 73.3 | 77.0 | 72.7 | 71.4 | 77.4 | 73.8 | 72.6 | 72.4 | 77.7 | 72.5 | 73.1 | 209.4 |
| 8 | 42.4 | 51.5 | 51.8 | 43.6 | 45.9 | 46.6 | 44.4 | 43.5 | 41.6 | 41.6 | 43.4 | 43.5 | 42.2 | 43.4 | 43.7 | 52.1 |
| 9 | 47.0 | 46.5 | 47.4 | 43.3 | 43.2 | 41.3 | 42.0 | 37.9 | 39.2 | 37.3 | 37.4 | 37.3 | 37.1 | 37.8 | 40.3 | 48.4 |
| 10 | 53.9 | 53.5 | 53.8 | 53.7 | 54.4 | 54.4 | 47.6 | 48.7 | 48.6 | 48.6 | 49.0 | 49.1 | 49.0 | 48.1 | 47.2 | 47.8 |
| 11 | 72.5 | 71.4 | 68.6 | 71.2 | 67.9 | 70.7 | 70.5 | 68.7 | 68.6 | 68.6 | 68.2 | 68.3 | 68.3 | 68.4 | 71.5 | 68.6 |
| 12 | 36.9 | 43.2 | 46.8 | 43.5 | 45.7 | 42.6 | 43.3 | 39.7 | 40.1 | 40.1 | 39.9 | 39.9 | 40.1 | 39.5 | 42.4 | 46.4 |
| 13 | 40.9 | 46.9 | 47.7 | 46.3 | 47.0 | 46.3 | 45.9 | 46.6 | 46.6 | 46.6 | 46.5 | 46.5 | 46.5 | 46.7 | 46.3 | 46.6 |
| 14 | 60.6 | 150.7 | 151.7 | 156.3 | 160.0 | 158.9 | 159.3 | 159.6 | 157.6 | 157.5 | 158.5 | 158.5 | 157.2 | 158.7 | 158.9 | 150.4 |
| 15 | 220.8 | 128.3 | 127.8 | 121.8 | 122.2 | 122.7 | 122.2 | 120.4 | 119.6 | 119.7 | 120.8 | 120.9 | 120.6 | 120.8 | 121.9 | 127.2 |
| 16 | 43.0 | 34.7 | 34.8 | 34.3 | 34.4 | 34.3 | 34.3 | 34.2 | 34.3 | 34.3 | 34.3 | 34.3 | 34.3 | 34.2 | 34.4 | 34.7 |
| 17 | 38.9 | 52.2 | 52.0 | 52.1 | 51.7 | 52.1 | 52.2 | 51.3 | 51.3 | 51.2 | 51.3 | 51.3 | 51.3 | 51.2 | 51.8 | 51.7 |
| 18 | 27.8 | 21.7 | 21.2 | 21.0 | 20.4 | 21.1 | 21.1 | 18.9 | 18.7 | 18.9 | 19.4 | 19.5 | 19.5 | 19.4 | 20.6 | 21.3 |
| 19 | 41.9 | 41.6 | 42.0 | 42.4 | 43.0 | 43.0 | 37.6 | 37.1 | 37.2 | 37.3 | 37.0 | 37.2 | 39.0 | 35.9 | 39.6 | 39.8 |
| 20 | 122.6 | 124.0 | 124.3 | 124.0 | 124.0 | 123.7 | 123.7 | 124.0 | 124.4 | 124.3 | 124.0 | 124.0 | 124.1 | 124.0 | 123.9 | 124.3 |
| 21 | 139.9 | 140.1 | 140.1 | 140.0 | 140.0 | 140.1 | 140.0 | 140.0 | 140.1 | 140.3 | 140.1 | 140.1 | 140.1 | 140.0 | 140.0 | 139.8 |
| 22 | 110.5 | 111.1 | 111.1 | 111.1 | 111.0 | 111.0 | 111.0 | 111.1 | 111.3 | 111.2 | 111.2 | 111.1 | 111.2 | 111.0 | 111.1 | 111.0 |
| 23 | 143.5 | 143.0 | 142.9 | 143.0 | 143.0 | 143.2 | 143.1 | 142.9 | 142.8 | 142.8 | 142.8 | 142.9 | 142.8 | 142.9 | 143.3 | 142.7 |
| 28 | 31.2 | 23.9 | 31.4 | 31.3 | 31.4 | 33.7 | 33.0 | 19.6 | 19.4 | 23.1 | 25.1 | 25.1 | 25.6 | 24.9 | 25.8 | 24.8 |
| 29 | 24.1 | 31.3 | 23.9 | 24.0 | 24.2 | 23.8 | 27.5 | 23.2 | 23.1 | 19.4 | 18.3 | 18.3 | 18.5 | 18.2 | 19.7 | 19.1 |
| 30 | 20.6 | 30.4 | 30.8 | 29.0 | 29.7 | 28.6 | 28.8 | 29.0 | 29.2 | 29.1 | 27.8 | 27.8 | 29.0 | 28.0 | 28.0 | 29.0 |
| 1′ | | | | | | | | 179.1 | 170.4 | 179.0 | 170.2 | 179.0 | 170.4 | | | 166.1 |
| 2′ | | | | | | | | 41.1 | 127.8 | 41.1 | 127.7 | 41.1 | 127.7 | | | 127.0 |
| 3′ | | | | | | | | 26.7 | 140.6 | 26.8 | 140.6 | 26.7 | 140.7 | | | 149.8 |
| 4′ | | | | | | | | 11.6 | 14.9 | 16.7 | 14.8 | 11.6 | 14.9 | | | 14.8 |
| 5′ | | | | | | | | 16.7 | 12.2 | 11.6 | 12.2 | 16.6 | 12.2 | | | 12.0 |
| 11-OAc | 21.6 | 21.5 | | 21.6 | | 21.6 | 22.4 | 21.3 | 21.3 | 21.3 | 21.7 | 21.8 | 21.6 | 21.8 | 21.5 | |
| 11-OAc | 170.1 | 170.4 | | 170.5 | | 170.5 | 170.8 | 169.9 | 170.4 | 170.4 | 170.0 | 170.2 | 170.1 | 172.8 | 169.8 | |
| 7-OAc | | | | 21.3 | | | | | 21.3 | 170.2 | 21.4 (6-OAc) | 21.4 (6-OAc) | 21.3 | 21.3 (6-OAc) | | |
| 7-OAc | | | | 169.8 | | | | | 170.0 | 21.3 | 170.0 (6-OAc) | 170.0 (6-OAc) | 171.7 | 170.3 (6-OAc) | | |

[a]NMR data (δ) were measured at 125 MHz in $CDCl_3$ for **1**–**16**.

the logarithmic phase were added to the chopped meat medium containing various concentrations of walrobsins in a 96-well plate. The final inoculum concentration of *P. acnes* was $1.25 \times 10^6$ CFU/mL. After incubation under anaerobic conditions for 24 h, the level of microbial growth was tested using a microplate reader at 600 nm. The MIC was defined as the lowest dilution of walrobsins at which growth was inhibited completely[20,21].

### 4.6. MTT assay

Effects of walrobsins **1–3**, **8–14**, and **19–20** on the viability of THP-1 cells were determined by the MTT method. Approximately $2 \times 10^5$ cells/well were seeded in 96-well plates and treated with different concentrations of walrobsins for 36 h (5% $CO_2$, 37 °C). Then, 20 μL MTT reagent (5 mg/mL) was added into the culture medium in each well accordingly. The formazan crystals were solubilized in 150 μL dimethyl sulfoxide after 4 h incubation. Absorbance was measured by a spectrophotometer at 570 nm excitation and 630 nm emission[20,21].

**Table 5** Anti-inflammatory activities of selective compounds on LPS-induced RAW 264.7, BV2 and *P. acnes* stimulated YHB-1. macrophages.

| No. | $IC_{50}$[a] | | |
|---|---|---|---|
| | RAW 264.7 | BV2 | THB-1 |
| **1** | >50 | >50 | >50 |
| **2** | 41.15±2.35 | 21.19±1.43 | >50 |
| **3** | >50 | >50 | >50 |
| **8** | 28.29±0.95 | 15.09±2.10 | 28.5±0.35 |
| **9** | 25.69±1.38 | 22.25±1.36 | 18.01±0.24 |
| **10** | >50 | >50 | >50 |
| **11** | 16.58±1.46 | 20.36±1.37 | 7.96±0.36 |
| **12** | >50 | >50 | >50 |
| **13** | 30.72±2.56 | NT[a] | 20.05±0.78 |
| **14** | 52.46±3.25 | >50 | 15.97±0.29 |
| **18** | 9.2±0.64 | NT | NT |
| **19** | 52.76±3.23 | >50 | >50 |
| **20** | >50 | >50 | >50 |
| L-NMMA[b] | 48.15±1.56 | >50 | NA |
| Retinoic acid[c] | NA | NA | 15.31±1.13 |

NT, not tested. NA, not applicable.
[a](μmol/L, mean±SD, $n = 3$).
[b]Positive control substance in RAW 264.7 and BV2 cell line.
[c]Positive control substance in THB-1 cell line.

### 4.7. Enzyme-linked immunosorbent assay

THP-1 cells ($2 \times 10^5$ cells/well) were cultured in 96-well plates in medium without FBS and incubated with different concentrations of walrobsins **1–3**, **8–14**, and **19–20** for 4 h. Then, THP-1 cells were stimulated by live *P. acnes* for 24 h and centrifuged to collect cell-free supernatants. The levels of IL-1$\beta$ in culture supernatants were measured with ELISA assays according to the instructions of manufacturer. Retinoic acid was used as the positive control[20,21].

### 4.8. Theoretical calculated ECD of 15

Theoretical calculations of ECD spectra for that of **15** were performed with the Gaussian 09 program package. The structure of **15** was optimized with MM2, and its geometry was re-optimized at the b3lyp/6–31g(d,p) level of theory. The ECD calculations of compound **15** were performed with DFT calculations at the b3lyp/6–311+g(d,2p) level of theory with 26 nm UV correction ($\sigma$=0.40). Detailed calculated parameters were proved in Supporting Information.

### 4.9. X-ray crystallography of 1

Single crystals of $C_{28}H_{35}O_7$ (**1**) were recrystallized from mixture solvent ($CH_2Cl_2$:MeOH=1:1, *v*:*v*). A suitable crystal was selected and recorded on a diffractometer using Cu K$\alpha$ radiation. The crystal was kept at 291(2) K during data collection. The structure was solved with the ShelXT structure solution program using Direct Methods and refined with the ShelXL refinement package using Least Squares minimisation based on Olex2 software[22]. The crystallographic data of compound **1** have been deposited at the Cambridge Crystallographic Data Center with the deposition number CCDC 1880306.

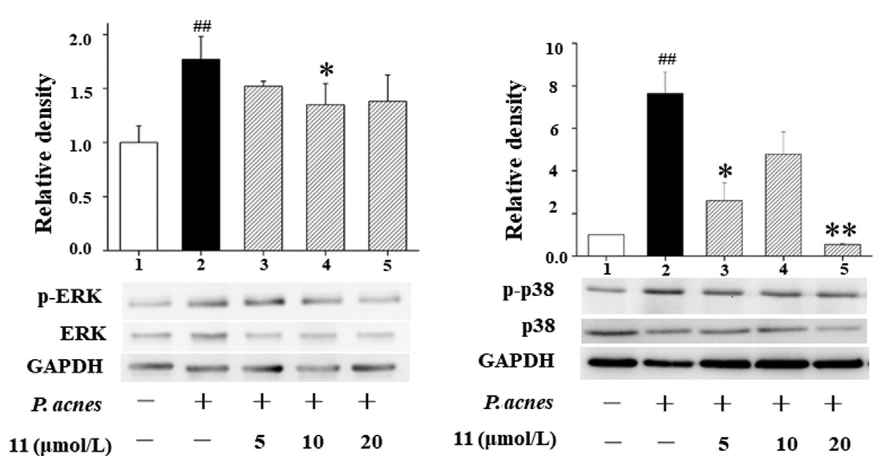


**Figure 8** Effects of **11** on the MAPK signaling pathway in *Propionibacterium ances*-stimulated THP-1 cells. The changes of ERK and p38 proteins were examined by Western blot. The data were in three independent experiments. $P<0.01$ compared to control cells; $^{**}P<0.01$ and $^{*}P<0.05$ compared to only *P. ances*-stimulated cells.

**Acknowledgments**

Financial support for this study by the National Natural Science Foundation of China (31470416, China), the Outstanding Youth Fund of the Basic Research Program of Jiangsu Province (BK20160077, China), the Program for Changjiang Scholars and Innovative Research Team in University (IRT_15R63, China), and the "Double First-Class" University project (CPU2018GY08, China).

**Appendix A. Supporting information**

Supplementary data associated with this article can be found in the online version at https://doi.org/10.1016/j.apsb.2019.02.009.

**References**

1. Guo Z. The modification of natural products for medical use. *Acta Pharm Sin B* 2017;**7**:119–36.
2. Tan QG, Luo XD. Meliaceous limonoids:chemistry and biological activities. *Chem Rev* 2011;**111**:7437–522.
3. Han ML, Shen Y, Wang GC, Leng Y, Zhang H, Yue JM. 11*β*-HSD1 inhibitors from Walsura cochinchinensis. *J Nat Prod* 2013;**76**:1319–27.
4. Ji KL, Zhang P, Hu HB, Hua S, Liao SG, Xu YK. Limonoids from the leaves and twigs of *Walsura yunnanensis*. *J Nat Prod* 2014;**77**:1764–9.
5. Luo XD, Wu SH, Ma YB, Wu DG. Tetranortriterpenoids from *Walsura yunnanensis*. *J Nat Prod* 2000;**63**:947–51.
6. Wang GC, Yu JH, Shen Y, Leng Y, Zhang H, Yue JM. Limonoids and triterpenoids as 11*β*-HSD1 inhibitors from *Walsura robusta*. *J Nat Prod* 2016;**79**:899–906.
7. Han ML, Shen Y, Leng Y, Zhang H, Yue JM. New rearranged limonoids from *Walsura cochinchinensis*. *RSC Adv* 2014;**4**:19150–8.
8. Nugroho AE, Okuda M, Yamamoto Y, Hirasawa Y, Wong CP, Kaneda T, et al. Walsogynes B–G, limonoids from *Walsura chrysogyne*. *Tetrahedron* 2013;**69**:4139–45.
9. Rao MS, Suresh G, Yadav PA, Prasad KR, Rani PU, Rao CV, et al. Piscidinols H–L, apotirucallane triterpenes from the leaves of *Walsura trifoliata* and their insecticidal activity. *Tetrahedron* 2015;**71**:1431–7.
10. An FL, Sun DM, Li RJ, Zhou MM, Yang MH, Yin Y, et al. Walrobsins A and B, two anti-inflammatory limonoids from root barks of *Walsura robusta*. *Org Lett* 2017;**19**:4568–71.
11. Zhang Y, An FL, Huang SS, Yang L, Gu YC, Luo J, et al. Diverse tritepenoids from the fruits of *Walsura robusta* and their reversal of multidrug resistance phenotype in human breast cancer cells. *Phytochemistry* 2017;**136**:108–18.
12. Yin S, Wang XN, Fan CQ, Liao SG, Yue JM. The first limonoid peroxide in the meliaceae family: walsuronoid A from *Walsura robusta*. *Org Lett* 2007;**9**:2353–6.
13. Zhou ZW, Yin S, Zhang HY, Fu Y, Yang SP, Wang XN, et al. Walsucochins A and B with an unprecedented skeleton isolated from *Walsura cochinchinensis*. *Org Lett* 2006;**10**:465–8.
14. Grkovic T, Pouwer RH, Vial ML, Gambini L, Noël A, Hooper JN, et al. NMR fingerprints of the drug-like natural-product space identify iotrochotazine A: a chemical probe to study parkinson's disease. *Angew Chem Int Ed* 2014;**53**:6070–4.
15. Liu Y, Zhou JL, Liu P, Sun S, Li P. Chemical markers' fishing and knockout for holistic activity and interaction evaluation of the components in herbal medicines. *J Chromatogr A* 2010;**1217**:5239–45.
16. Song HP, Wu SQ, Qi LW, Long F, Jiang LF, Liu K, et al. A strategy for screening active lead compounds and functional compound combinations from herbal medicines based on pharmacophore filtering and knockout/knockin chromatography. *J Chromatogr A* 2016;**1456**:176–86.
17. Jiang L. Three tetranortriterpenoids from *Walsura yunnanensis*. *Chem Nat Compd* 2013;**48**:1013–6.
18. O'Boyle NM, Vandermeersch T, Flynn CJ, Maguire AR, Hutchison GR. Confab-systematic generation of diverse low-energy conformers. *J Cheminform* 2011;**3**:8.
19. Li RJ, Gao CY, Guo C, Zhou MM, Luo J, Kong LY. The anti-inflammatory activities of two major withanolides from *Physalis minima via* acting on NF-*κ*B, STAT3, and HO-1 in LPS-stimulated RAW264.7 cells. *Inflammation* 2017;**40**:401–13.
20. Guo MM, An FL, Yu HY, Wei X, Hong MH, Lu YH. Comparative effects of schisandrin A, B, and C on *Propionibacterium acnes-induced*, NLRP3 inflammasome activation-mediated IL-1*β* secretion and pyroptosis. *Biomed Pharmacother* 2017;**96**:129–36.
21. Guo MM, An FL, Wei X, Hong MH, Lu YH. Comparative effects of schisandrin A, B, and C on acne-related inflammation. *Inflammation* 2017;**40**:2163–72.
22. Dolomanov OV, Bourhis LJ, Gildea RJ, Howard JAK, Puschmann H. *J Appl Cryst* 2009;**42**:339–41.